Nonlinear finite element analysis of reinforced concrete beam-column joints under reversed cyclic loading

PAPER • **OPEN ACCESS**

Nonlinear finite element analysis of reinforced concrete beam-column joints under reversed cyclic loading

To cite this article: A Tambusay *et al* 2020 *IOP Conf. Ser.: Mater. Sci. Eng.* **930** 012055

IOP Conf. Series: Materials Science and Engineering **930** (2020) 012055 doi:10.1088/1757-899X/930/1/012055

Nonlinear finite element analysis of reinforced concrete beam-column joints under reversed cyclic loading

A Tambusay[1,2], B Suryanto[1]* and P Suprobo[2]

[1] Institute for Infrastructure and Environment, School of Energy, Geoscience, Infrastructure and Society, Heriot-Watt University, Edinburgh, United Kingdom.
[2] Department of Civil Engineering, Faculty of Civil, Planning and Geo Engineering, Sepuluh Nopember Institute of Technology, Surabaya, East Java, Indonesia.

*Corresponding author's e-mail: B.Suryanto@hw.ac.uk

Abstract. This paper presents the application of three-dimensional nonlinear finite element analysis in studying the complex behaviour of reinforced concrete beam-column joints under reversed cyclic loading. Three different joint types were considered: an interior, an exterior, and a corner joint, each representing typical joint configurations in general moment resisting frame structures. These joints' test data were taken from the experimental investigations carried out by Shiohara and Kusuhara about 15 years ago and used here to showcase the practical application and value of an advanced numerical modelling. It is shown that the numerical models are able to accurately capture the full cyclic hysteretic response, progressive strength and stiffness degradation, cracking and damage evolution under load cycles, and failure mode. It is also shown that the numerical models provide a useful tool to characterise failure processes and behavioural mechanisms.

1. Introduction

Beam-column joint is widely considered as a critical element in reinforced concrete moment-resisting frame structures [1]. When subjected to earthquake-induced lateral forces, premature failure can occur in a poorly detailed joint element [1-5] and this failure can be very brittle as in concrete beams with little or no shear reinforcement [6-9]. Joint shear failure can also occur in overly reinforced concrete beams as flexural yielding cannot be achieved due to high ratio of longitudinal steel bars [10].

The key to ensuring the ductility and inelastic deformability of a beam-column joint depends primarily on the ability of the joint to sustain high shear stresses, particularly when flexural cracks have developed within the plastic hinge regions of the adjoining beams. In any case, it must be ensured that the columns remain essentially elastic throughout the load history to ensure global structural stability. This behavioural response is generally aimed for in the design as it will allow for inelastic large deformation to occur in the beams while preventing premature joint failure. A considerable amount of work [11-13] has been devoted since early 1960s to study the behaviour of beam-column joints under load reversals departing from the above concept and a number design recommendations have since been developed to ensure adequate connection behaviour in frame structures.

In the current building codes for beam-column joints [14, 15], a strength-based approach is generally adopted with joint shear strength typically being determined to meet the factored force demands imposed by adjoining members (i.e. beams and columns). By doing so, a joint can be expected to behave satisfactorily during load (shear) reversals. Provisions in a strong column-weak beam, anchorage length

of longitudinal bars, and adequate shear reinforcements are also given to ensure the integrity of a structure in the post-yielding region. Although the ultimate stage limits are provided to protect against loss of lives and structural collapse, the formation of wide diagonal cracks in the joint can still occur [16].

Apart from the design point of view, the mechanics of a beam-column joint under load reversals have also presented a major challenge to finite element modellers, particularly those implementing the smeared approach as stresses could be highly localised. The difficulty is partly due to the highly complex behaviours and involvement of many interrelated factors, including the flexural actions from both beams and columns, joint shear response, bond-slip effects, and joint concrete confinement. To investigate these aspects, Shiohara and Kusuhara [17, 18] performed extensive experimental investigations on reinforced concrete beam-column joints, with the aim at providing reliable test data for model verifications. In their study, three loading types were considered to simulate typical boundary conditions in a structure i.e. (i) an interior, (ii) an exterior, and (iii) a corner beam-column joint. The results of their experiments have since been used as the subject for further studies and generally treated as a benchmark data for verifying the accuracy of nonlinear finite element procedures.

In this paper, the practical value and application of three-dimensional nonlinear finite element analysis is demonstrated through accurate simulations of the cyclic hysteretic responses of beam-column joints along with crack patterns. The beam-column joints tested by Shiohara and Kusuhara [17] were selected as a benchmark to testify the accuracy of the finite element analyses. A combination of plasticity and fracture model in conjunction with a smeared fixed crack approach and crack band model was adopted to this end.

2. Details of Shiohara and Kusuhara Beam-Column Joints

In 2006, Shiohara and Kusuhara [17] undertook a detailed experimental programme on six half-scale beam-column joints (hereinafter referred to as the SK beam-column joints). The primary objective of the test programme was to provide benchmark test data for the validation of their in-house mathematical models. Due to the high quality and comprehensive documentation of test results, their test data have been referred to by many researchers and used to support the corroboration in many software developments [19, 20].

In this paper, only one series (series A) of the three series of SK beam-column joints was analysed. In this series, there were three specimens (labelled A1, A2 and A3), each of which was tested under different loading patterns to cover possible types of beam-column joint in moment-resisting frame buildings. All specimens in this series are of critical form and were designed as per AIJ guidelines [21]. Loading type I was intended to simulate an interior joint and this was applied to specimen A1 to address significant joint core distress. Loading types II and III were intended to simulate an exterior and corner joint, respectively, and applied to specimens A2 and A3 (these are the specimens that sustained the least joint core distress). The joint shear capacity of specimen A1 was designed to be 10% higher than the joint shear demand. The strong column-weak beam concept was considered, with an overstrength factor of 1.25 to allow the beams to achieve their full flexural capacities prior to the columns.

The typical schematic representations of all beam-column joints geometry and reinforcement layout are displayed in figure 1(a), together with the schematic of the test setup in figures 1(b)-(d). All beam-column joints had a similar square section of 300 by 300 mm and were reinforced with steel bars of identical arrangement and properties (see table 1). The concrete used to cast these specimens had the mean compressive and tensile splitting strengths of 28.3 MPa and 2.67 MPa, respectively. The specimen details are summarised in table 2.

Table 1. Material properties of reinforcing bars in series A specimen [17].

Diameter (mm)	Grade	Young's Modulus (GPa)	Yield Strength (MPa)	Ultimate Strength (MPa)
13[a]	SD390	176	456	582
13[b]	SD390	176	357	493
6	SD295	151	326	488

Notes: a: steel bar used for beams; b: steel bar used for columns

Table 2. Details of SK beam-column joint specimens [17].

Description		A1	A2	A3
Model		Interior	Exterior	Corner
Loading type		I	II	II
Compressive strength of concrete		28.3 MPa		
Beams	Cross-section	300 × 300 mm		
	Span	2700 mm		
	Longitudinal bar	8D13 (top) and 8D13 (bottom)		
	Transverse bar	D6 at 50 mm		
Columns	Cross-section	300 × 300 mm		
	Height	1470 mm		
	Longitudinal bar	16D13		
	Transverse bar	D6 at 50 mm		
Joint	Transverse bar	D6 at 50 mm (3 NoS)		

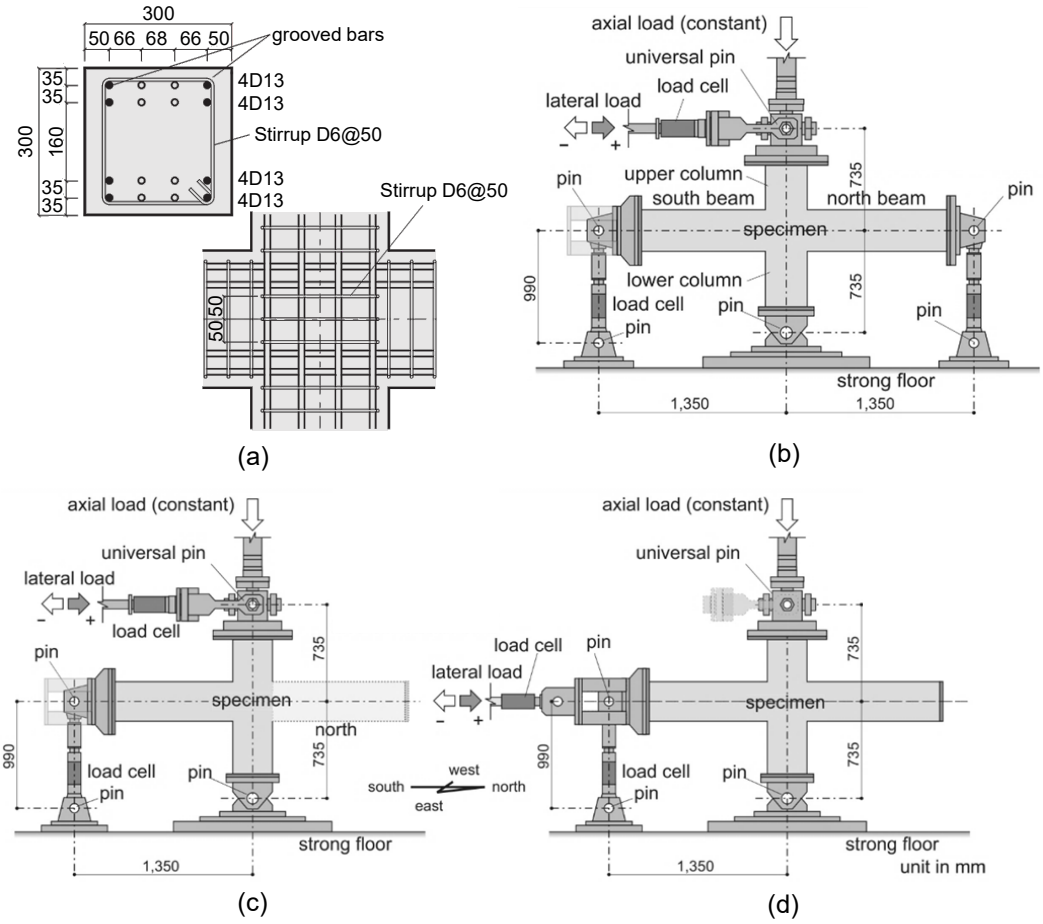

Figure 1. Schematic of series A of SK beam-column joints: (a) cross-section and bar arrangement; (b) loading type I; (c) loading type II; and (d) loading type III [17].

3. Finite Element Model

Three-dimensional nonlinear finite element analyses were performed using a specialist finite element software package ATENA Science developed exclusively by Červenka Consulting [22] for simulations of reinforced concrete structures [23, 24]. In this study, the accuracy of a smeared fixed crack approach to model the highly nonlinear cracked concrete behaviours experiencing bi-directional cracking [25, 26] resulting from reversed cyclic loads is tested. Figures 2(a) and (b) display the typical finite element

meshes and bar arrangements used to represent SK beam-column joints, which was prepared in a pre-processor finite element software GiD. The concrete was modelled using 8-node hexahedral (brick) linear elements with a typical size of 25 mm (in columns, beams and joint region), thereby giving 12 elements across the overall depth or width. All plates were modelled using tetrahedral linear elements with larger unstructured mesh size as a means to expedite the runtime of analysis. Although different mesh sizes were used for the concrete and steel (end) plates, this would not affect the accuracy as there is a full compatibility between two mesh surfaces.

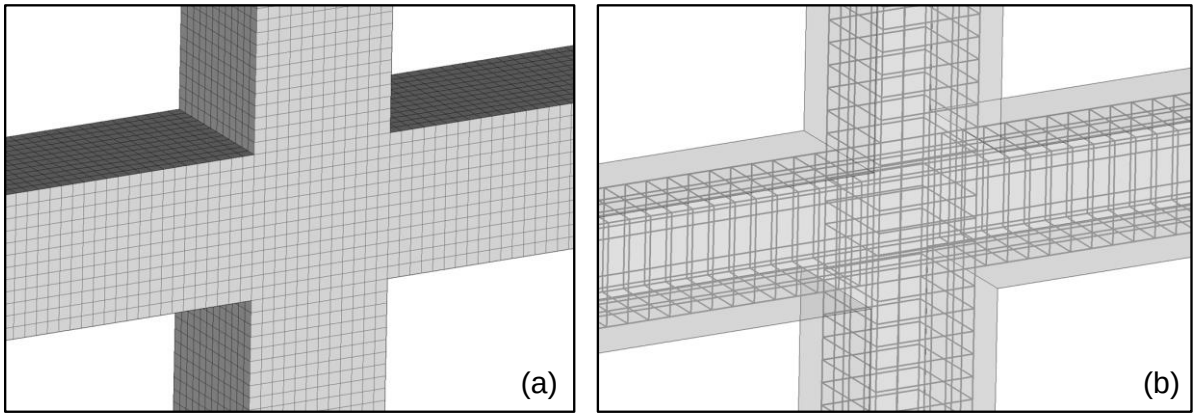

Figure 2. (a) Finite element mesh and (b) bar arrangement in ATENA Science.

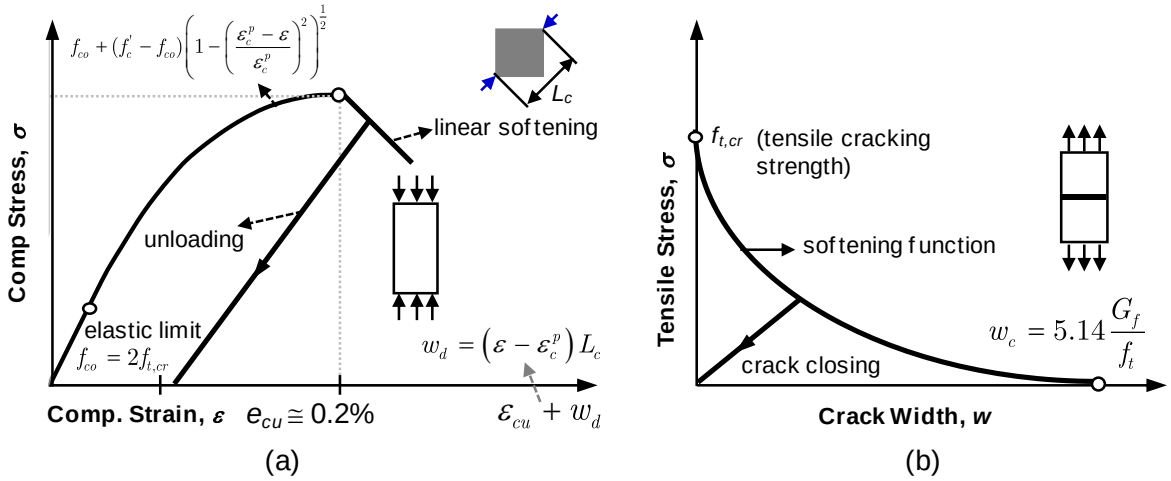

Figure 3. Concrete constitutive model: (a) compression and (b) tension.

The nonlinear concrete used in this study was the "Cementitious2" model which was formulated based on the CEB-FIP Model Code 1990 [27]. In this model, the response in compression is treated following the theory of plasticity, whereas the response in tension is formulated following the Rankine fracturing model for concrete cracking [22]. In the shear model, a constant shear factor coefficient (S_F), which defines a relationship between normal and shear (both modes II and III) crack stiffnesses, was used. Figures 3(a) and (b) show a summary of the constitutive laws adopted in this study. To model concrete behaviour under cyclic loading, the unloading factor parameter was activated to control the crack closure stiffness. In ATENA, this parameter can be set between 0 and 1, with 0 for unloading to the origin (default value for backward compatibility) and 1 for unloading parallel to the initial elastic stiffness. In this work, this factor was set to 0.2 and found to simulate residual displacement during unloading reasonably. Apart from this, the plastic flow was modified to a value of 0.5 to account for dilatancy resulting from the concrete volumetric expansion when undergoing compression failure.

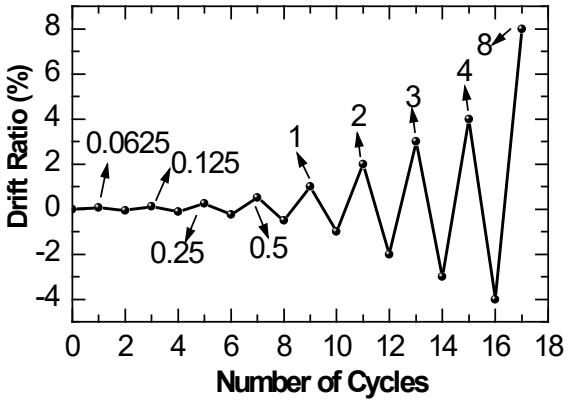

Figure 4. Loading history for reversed cyclic loading

Table 3. Summary of material parameters and finite element input parameters in ATENA.

No	Parameter	Value/Reference
Concrete constitutive model		
1.	Elastic modulus	CEB-FIP Model Code [27]
2.	Tensile strength	CEB-FIP Model Code [27]
3.	Smeared crack model	1 (fixed crack)
4.	Aggregate size	20 mm
5.	Unloading factor for cyclic loading	0.2
6.	Critical compressive displacement	0.5 mm
7.	Limit of comp. strength reduction due to cracking	0.8
8.	Eccentricity (defining the shape of failure surface)	0.52
9.	Plastic flow (defining dilatancy of plastic factor)	0.5
Reinforcement bar model		
10.	Stress-strain relationship	Bilinear with strain hardening
11.	Bond-slip model for cyclic (bar with memory bond)	CEB-FIP Model Code [27]
12.	Cyclic behaviour (Menegotto-Pinto)	R = 10; C1 = 0.925; and C2 = 0.15 [28]
Loading procedure and solution parameter		
13.	Loading procedure for axial load	Static (force-controlled)
14.	Loading procedure for cyclic load reversal	Quasi-static (displacement-controlled)
15.	Iteration method for cyclic	Modified Newton-Raphson
16.	Stiffness type	Elastic predictor with conditional break criteria
17.	Iteration limit	300
18.	Solver	Pardiso

All embedded steel bars were modelled in discrete representation using one-dimensional 2-noded linear truss elements. Elasto-plastic Manegotto-Pinto model [28] was used to accurately capture the cyclic behaviour of steel bars as it takes into account the Bauschinger's effect during unloading and reloading sequences. Bond-slip with memory bond was also considered following the nonlinear bond-slip formulation in the CEB-FIP Model Code 1990 [27].

In all models, the lower column was supported by a pin-joint. In the first loading interval, each beam-column joint was loaded with a constant axial load of 216 kN at the top of the upper column. In the second and subsequent intervals, cyclic lateral loads were then applied in the form of displacement increments, with a rate of 1.0 mm per step until reaching the drift ratio of 8% (see figure 4). For loading type I (specimen A1), the interior beam-column joint was supported at both sides of beam ends (with a pin and a roller support respectively) and the cyclic lateral loads were then applied at the top of the upper column. For loading type II (specimen A2 or an exterior beam-column joint), the lateral loads were applied in the same manner to that applied in loading type I – however, only one side of the beams was supported by a roller; accordingly, no internal stresses would develop in the other (dummy) beam. For

loading type III (specimen A3 or a corner beam-column joint), the analysis was done by applying cyclic lateral loads at one of the beam ends. The support conditions were similar to that of loading type II.

In this study, the modified Newton-Raphson iterative solution parameter with elastic predictor was used to allow for consistent convergence at each of load steps. Input parameters in conditional break criteria were set higher than that of default values, typically ten times higher to provide more space when convergence difficulties are encountered. The convergence tolerance was set constant throughout intervals with a value of 1.0% for displacement, residual, and absolute residual error, whilst energy error was set at 0.1%. High iteration limits (e.g. 200-300) were found to be beneficial. The key input parameters used in the analyses are summarised in table 3.

4. Results and Discussion

4.1. Hysteretic response

Figures 5(a)-(c) display the load-drift responses for specimens A1 to A3, with a summary of the measured and predicted load capacities presented in table 4. As shown in the figures, the overall behaviours of the beam-column joints can be predicted reasonably well. The finite element models successfully exhibit comparable hysteretic shapes, particularly for specimens A2 and A3 which display similar response as observed in the experiment.

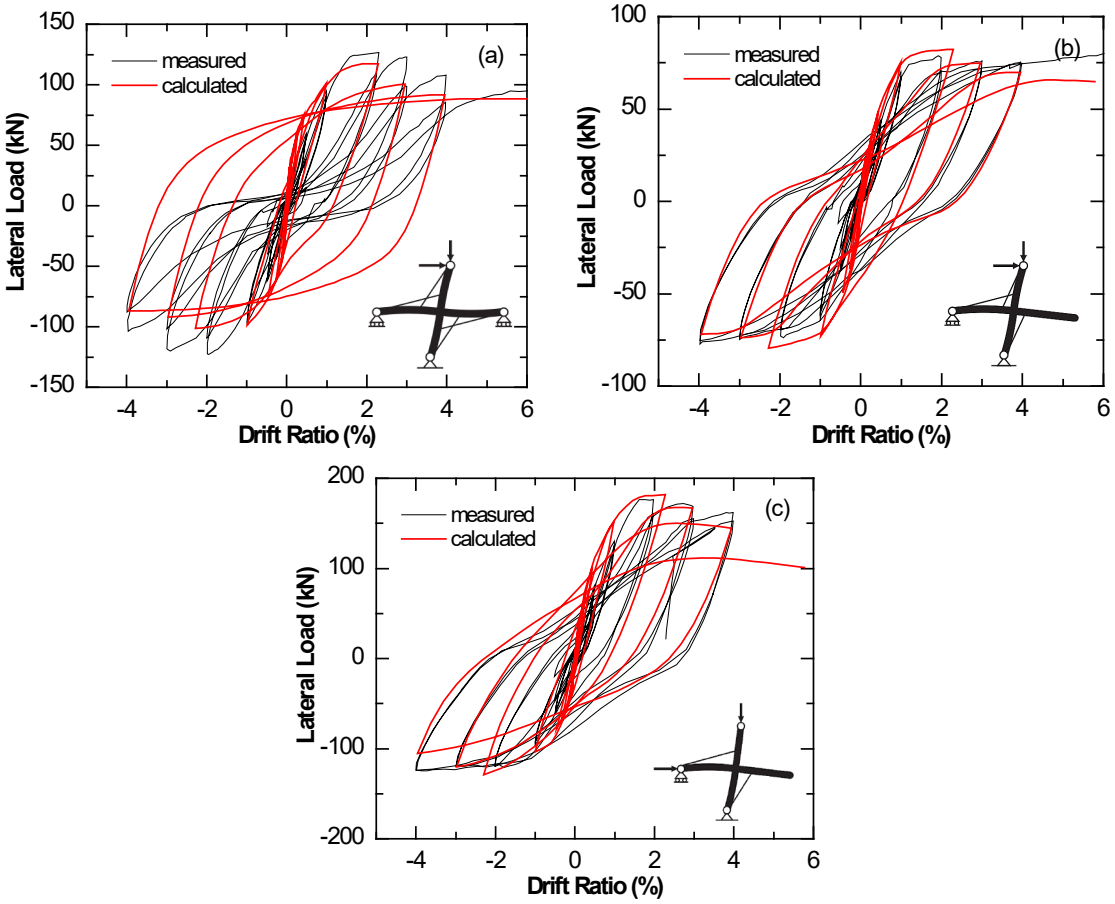

Figure 5. Loading history under reversed cyclic loading. Test data were taken from [17].

With regard to the response of interior beam-column joint (specimen A1), it is apparent from figure 5(a) that at low drift levels, the predicted hysteretic response displays accurate representation of strength and stiffness degradation. As the drift is increased further, however, the analysis starts to slightly underestimate the load capacity (particularly from the 5th cycle), but the agreement is still reasonable. Of interest to note is the overly high total energy dissipation in the analysis due to the more rounded

shape of hysteretic loops during load cycles (compared to the highly pinched response). This could also be attributed to high complexity of joint distress incurred by the specimen, thereby making it difficult to predict with accuracy. As shown in table 4, the ratios of experimental-to-predicted load capacity for specimen A1 in the positive and negative loading direction are 1.08 and 1.16 respectively.

Table 4. Summary of experimental [17] and predicted load capacities.

Joint Specimen	Positive Loading Direction			Negative Loading Direction		
	$P_{u\text{-}Test}$ (kN)	$P_{u\text{-}Calc}$ (kN)	$P_{u\text{-}Test}/P_{u\text{-}Calc}$ (-)	$P_{u\text{-}Test}$ (kN)	$P_{u\text{-}Calc}$	$P_{u\text{-}Test}/P_{u\text{-}Calc}$ (-)
A1	126.6	117	1.08	-122.8	-106	1.16
A2	77.9	82	0.95	-77.1	-79	0.98
A3	176.4	182	0.97	-124.5	-129	0.97
		Mean	1.00		Mean	1.03
		CoV (%)	5.82		CoV (%)	9.46

Figures 5(b) and (c) compare the measured and predicted hysteretic responses for specimens A2 and A3 respectively. An excellent agreement is observed in terms of initial stiffness, load capacity, and the overall shape of the hysteretic loops. The strength and stiffness degradation can also be predicted with accuracy, although there is a slight variation of strength degradation during the 8th cycle which corresponds to the drift ratio of 4%. It is noteworthy that the models can better replicate the hysteretic shapes for specimens with less joint core distress. The ratios of experimental-to-predicted load capacity for specimens A2 and A3 in the positive and negative loading direction are 0.95/0.98 (A2) and 0.97/0.97 (A3) respectively which is indicative of marginal differences (consistently less than 5%), highlighting the excellent accuracy of finite element predictions.

4.2. Comparison of crack patterns

To facilitate further evidence of the accuracy of finite element models used in this study, figures 6-8 compare the observed and predicted crack patterns at selected drift ratio levels of 0.5%, 2%, and 4%. It is evident that, in general, the overall predicted crack patterns are in excellent agreement with the observed crack patterns in terms of the extent of accuracy of crack-alike development, location of crack, and mode of failure. The successful representation of crack angle (also principal strain profile) in all specimens under increasing loads is also appealing, highlighting once again successful appreciation of the highly nonlinear behaviours of the concrete by the finite element models.

With reference to the cracking behaviour of specimen A1, it is apparent that under load reversals, flexural cracks initially develop at the beam corners at the joint and then propagate diagonally within the joint core which is indicative of shear cracks. These existing shear cracks, during the increasing load levels, progress significantly within the joint, replicating more to a typical concrete strut action. The reason for this relates to the low overstrength factor of joint shear capacity (10%) as reported by Shiohara and Kusuhara [17]. At a drift ratio of 4%, shear cracks start to develop within the plastic hinge regions of both lower and upper columns. This is attributed to the marginal value of the overstrength factor in the strong column-weak beam design (i.e. 1.25). Therefore, it is not surprising that joint core exhibits heavy shear distress followed by diagonal concrete crushing, while the columns also experience significant damage. Furthermore, the analysis clearly shows that the longitudinal bars in the beams have reached their yield capacities, as evidenced by considerable flexural cracks formation along the beam length.

With respect to specimens A2 and A3, the failure modes are predicted to be flexure-shear in nature which is consistent with experimental observation. Significant flexural cracks manifest vastly in one side of the beam, following the formation of shear cracks in the joint core. In this specimen, damage is dominated primarily by flexural cracks with no existence of concrete crushing. It is interesting to note that in specimen A2 (exterior beam-column joint), concrete cracking is shown to develop primarily in the beam and within the joint core, whereas in specimen A3 (a corner or knee joint), concrete cracking is shown to also manifest in the lower column at locations within the plastic hinge region.

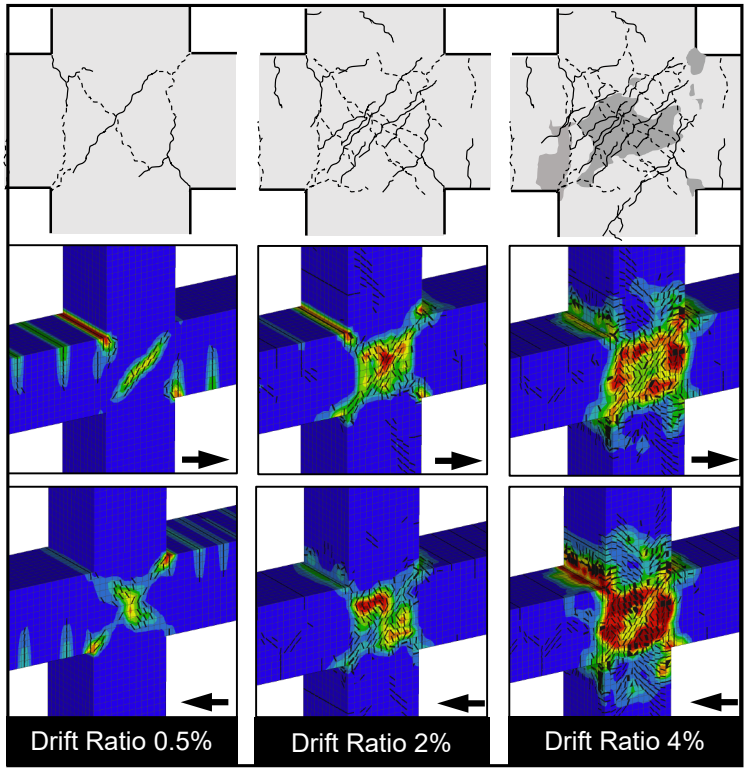

Figure 6. Computed and observed crack patterns and maximum principal strains of specimen A1.

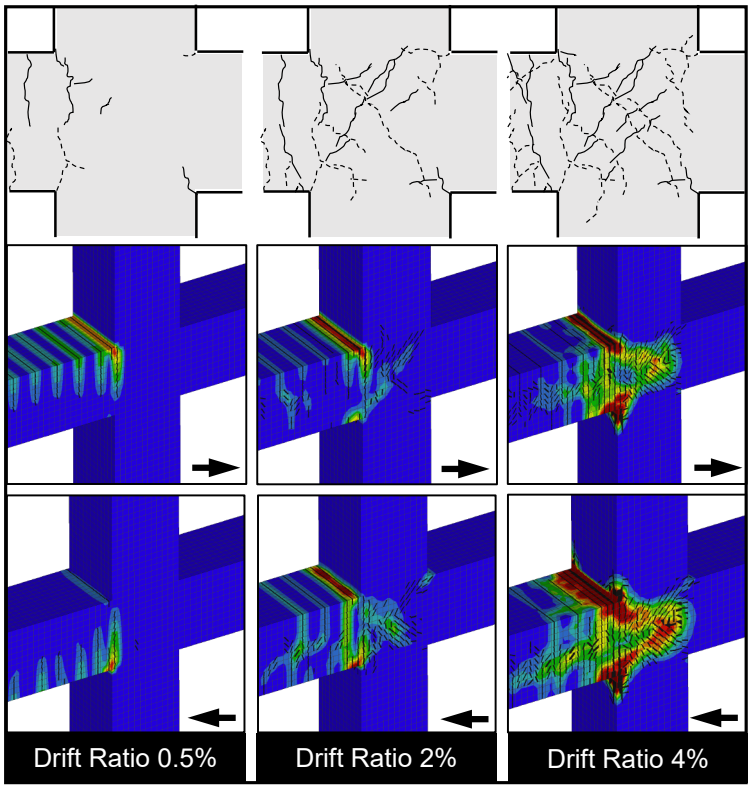

Figure 7. Computed and observed crack patterns and maximum principal strains of specimen A2.

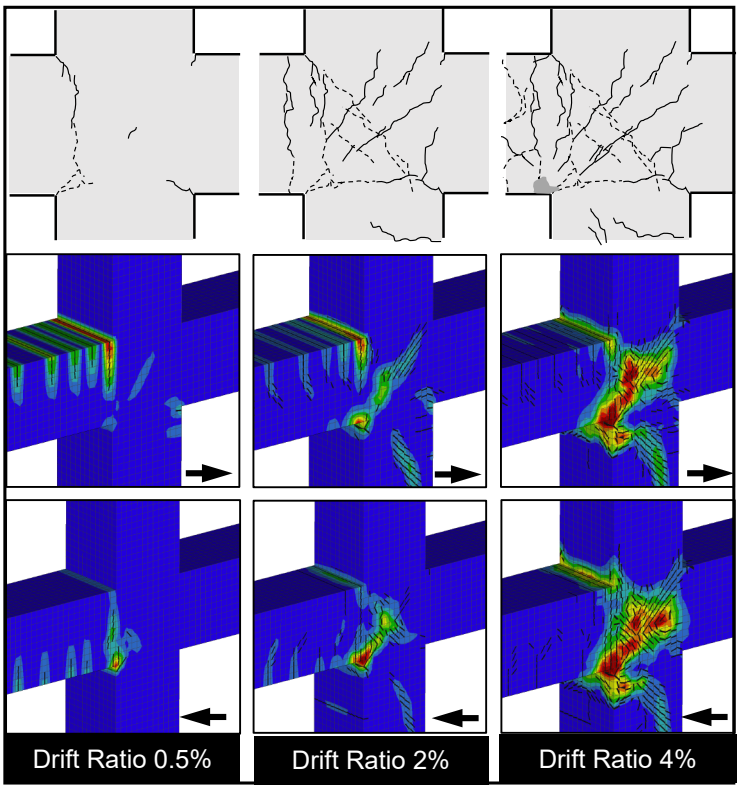

Figure 8. Computed and observed crack patterns and maximum principal strains of specimen A3.

5. Concluding remarks and conclusions

The application of three-dimensional nonlinear finite element analyses using ATENA Science is presented, with the models prepared using a pre-processor software GiD. Three beam-column joints tested by Shiohara and Kusuhara, representing the interior, exterior and corner joints, were thoroughly modelled and simulated under quasi-static displacement-controlled load reversals. The fracture-plastic model employing the classical path-dependent smeared crack formulation and crack band model was adopted to showcase the applicability of this approach for complex simulations of reinforced concrete under cyclic loading. This work also aims to respond to the need for establishing an appropriate modelling strategy under cyclic loading which still presents challenges to finite element modellers.

Based on the analytical work presented, some conclusions are drawn:

1. The use of ATENA Science is shown to provide good capabilities to simulate multifaceted nonlinear behaviour of beam-column joints under cyclic lateral loads. The nonlinear material models implemented in the software is shown to produce hysteretic loops and crack profiles which are in excellent agreement with experimental observations.
2. It is shown that the load capacity of the joints can be well predicted, with the predictions slightly underestimating the load capacity of the interior joint and slightly overestimating the load capacities of the exterior and corner joints. The computed crack patterns display good representation of the test data, with similar crack development demonstrated across the members. Accurate predictions of failure modes were also obtained.
3. The extent of damage in the analysis is shown to compare well with the actual damage in the test specimens. This is particularly true for the interior joint which is generally more critical and subjected to large shear stresses. The results demonstrate the suitability of reliable simulations to tackle challenges in predicting damage level under day-to-day design.

The analysis tool discussed in this paper can provide practising engineers and researchers with the ability to assess detailed behavioural response of structural elements subjected to unforeseen loading conditions such as earthquake. It could also be a useful tool in the assessment of structural elements with unusual detailing, particularly if constructed in seismic prone area.

Acknowledgements
This work was supported by an Institutional Links grant, ID 414707757, under the Newton Fund Institutional Links Grant and the Ministry of Research, Technology and Higher Education of the Republic of Indonesia partnership. The grant is funded by the UK Department for Business, Energy and Industrial Strategy and the Indonesian Ministry of Research, Technology and Higher Education (Grant No. 3/AMD/EI/KP.PTNBH/2020) and delivered by the British Council. The authors would also express their gratitude to Dr. Jan Červenka for his valuable discussions.

References
[1] Sharma A, Eligehausen R and Reddy G R 2011 A new model to simulate joint shear behavior of poorly detailed beam-column connections in RC structures under seismic loads–part 1: exterior joints *Eng. Struc.* **33** 3 1034–51
[2] Li B, Wu Y and Pan T C 2002 Seismic behavior of nonseismically detailed interior beam-wide column joints–part I: experimental results and observed behavior *ACI Struc. J.* **99** 2 791–802
[3] Li B, Wu Y and Pan T C 2003 Seismic behavior of nonseismically detailed interior beam-wide column joints–part II: theoretical comparisons and analytical studies *ACI Struc. J.* **100** 1 56–65
[4] De Risi M T, Ricci P, Verderame G M and Manfredi G 2016 Experimental assessment of unreinforced exterior beam-column joints with deformed bars *Eng. Struc.* **112** 215–32
[5] Hwang S-J, Lee H-J, Liao T-F, Wang K-C and Tsai H-H 2005 Role of hoops on shear strength of reinforced concrete beam-column joints *ACI Struc. J.* **102** 3 445–53
[6] Collins M P, Bentz E C and Sherwood E G 2008 Where is shear reinforcement required? Review of research results and design procedures *ACI Struc J.* **105** 5 590–600
[7] Suryanto B, Morgan R and Han A L 2016 Predicting the response of shear-critical reinforced concrete beams using response-2000 and SNI 2847:2013 *Civ. Eng. Dimens.* **18** 1 16–24
[8] Suryanto B, Tambusay A and Suprobo P 2017 Crack mapping on shear-critical reinforced concrete beams using an open source digital image correlation software *Civ. Eng. Dimens.* **19** 2 93–8
[9] Tambusay A, Suryanto B and Suprobo P 2018 Visualization of shear cracks in a reinforced concrete beam using the digital image correlation *Intr. J. Adv. Sci. Eng. Inf. Tech.* **8** 1 573–8
[10] Ghobarah A and Said A 2002 Shear strengthening of beam-column joints *Eng. Struc.* **24** 881–8
[11] Hanson N W and Connor H W 1967 Seismic resistance of reinforced concrete beam-column joints *J. Struc. Div.* **93** 5 533–60
[12] Hanson N W 1971 Seismic resistance of concrete frames with grade 60 reinforcement *J. Struc. Div.* **97** 6 1685–700
[13] Megget L M and Park R 1971 Reinforced concrete exterior beam-column joints under seismic loading *New Zaeland Eng.* **26** 11 341–53
[14] AIJ 2016 Standard for lateral load-carrying capacity calculation of reinforced concrete structures *Architectural Institute of Japan* (Tokyo: Japan)
[15] ACI 318-19 2019 Building code requirements for structural concrete and commentary *American Concrete Institute* (Michigan: United States of America)
[16] Parra-Montesinos G J, Peterfreund S W and Chao S H 2005 Highly damage-tolerant beam-column joints through use of high-performance fiber-reinforced cement composites *ACI Struc. J.* **102** 3 487–95
[17] Shiohara H and Kusuhara F 2006 Benchmark test for validation of mathematical models for non-linear and cyclic behavior of R/C beam-column joints *The University of Tokyo* (Tokyo: Japan).
[18] Kusuhara F and Shiohara H 2008 Test of R/C beam-column joint with variant boundary conditions and irregular details on anchorage of beam bars *Int. Proc. 14th World Conf. Earth. Eng.* (Beijing: China)

[19] Guner S and Vecchio F J 2010 Analysis of shear-critical reinforced concrete plane frame elements under cyclic loading *J. Struc. Eng.* **137** 8 834–43
[20] Pan Z, Guner S and Vecchio F J 2017 Modeling of interior beam-column joints for nonlinear analysis of reinforced concrete frames *Eng. Struc.* **142** 182–91
[21] AIJ 1999 Design guidelines for earthquake resistant reinforced concrete building based on inelastic displacement concept *Architectural Institute of Japan* (Tokyo: Japan)
[22] Červenka V, Jendele L and Červenka J 2018 Program documentation ATENA theory Czech Republic, Červenka Consulting
[23] Tambusay A and Suprobo P 2019 Predicting the flexural response of a reinforced concrete beam using the fracture-plastic model *J. Civ. Eng.* **34** 2 61–7
[24] Červenka J, Červenka V and Laserna S 2018 On crack band model in finite element analysis of concrete fracture in engineering practice *Eng. Fract. Mech.***197** 27–47
[25] Suryanto B, Nagai K and Maekawa S 2010 Modeling and analysis of shear-critical ECC members with anisotropy stress and strain fields *J. Adv. Conc. Techn.* **8** 2 239–58
[26] Suryanto B, Nagai K and Maekawa S 2010 Smeared-crack modeling of R/ECC membranes incorporating an explicit shear transfer model *J. Adv. Conc. Techn.* **8** 3 315–26
[27] CEB-FIP Model Code 1990 Comité Euro-International du Béton *Inf. Bullet.* **195**
[28] Menegotto M and Pinto P E 1973 Method of analysis of cyclically loaded RC plane frames including changes in geometry and non-elastic behavior of elements under combined normal force and bending *IABSE Symp.* (Lisbon: Portugal) pp 15–22